MONTE CARLO STUDY OF A MONOMOLECULAR FILM OF A CHEMICALLY ASSOCIATING POLYMERIZING FLUID ADSORBED ON CRYSTALLINE LATTICES

Yu. Duda[1,*], O. Pizio[1], S. Sokolowski[2], N. Batina[3]
[1] *Instituto de Química de la UNAM, Circuito Exterior, Coyoacán 04510, México, D.F.*
[2] *Computer Laboratory, Faculty of Chemistry, Marie Curie–Sklodowska University, 200–31 Lublin, Poland*
[3] *Departmento de Fisica, Universidad Autonoma Metropolitana/Iztapalapa, 09430, Mèxico, Distrito Federal*
[*] *Permanent address: Institute for Condensed Matter Physics, National Academy of Sciences of Ukraine, Lviv–11, Ukraine*

(Received March 3, 1998)

We consider a model for a monomolecular film of a polymerizing fluid adsorbed on a crystalline surface and study it using NVT Monte Carlo simulations. The model represents a two–dimensional chemically associating fluid of hard discs with center–center repulsion and site–site attraction, such that with increasing association energy discs polymerize in the external heterogeneous field due to a crystalline surface. It is shown that both the valence angle between attractive sites and the association energy influence the monolayer structure. We have performed a comparison of the results for the homogeneous surface (Yu. Duda et al., J. Coll. Interface Sci. **194**, 68 (1997)) and the (100) single crystal plane is chosen to elucidate the effect of a substrate crystalline symmetry on the polymerization of species. Analysis of complexes that are formed due to association in terms of the fractions of singly and doubly bonded particles, of average numbers of chains and rings and of their size is presented. The average end to end distance, the radius of gyration and the persistence length of the products of polymerization are calculated. The dependencies of the monolayer structure on density, on the fluid–solid energy and on the valence angle are investigated.

Key words: monolayers, polymerizing fluids, two–dimensional model, crystalline lattice.

PACS number(s): 61.20.Qg, 82.30.Nr, 61.25.Em, 61.25.Hq

I. INTRODUCTION

There is currently a considerable interest in highly ordered monomolecular adlayers on solid surfaces for basic research, as well as for technological applications. In particular, the studies of monomolecular layers of chain molecules using the scanning tunneling microscopy have received much experimental attention [1–6]. Single crystal surface as well as modified surfaces have been used in those experiments as a substrate.

Previous theoretical investigations of monolayer adsorption mostly apply to ideal surfaces and to simple fluid models in two dimensions (2D), such as hard discs, Lennard–Jones discs, planar dumbbells, see e.g. [7–13]. Very recently, Zhou, Hall and Stell have attempted to develop a thermodynamic perturbation theory of 2D fused hard–disc chain fluids [13]. These authors have emphasized necessity to accumulate simulation data for the development of the theory of 2D complex fluids.

We have initiated the study of 2D chemically associating fluids in our recent works [14–16], using Monte Carlo simulations and integral equations. In the present work we consider a 2D model for *polymerization* of particles via *directional* bonding in a monolayer adsorbed on a *crystalline* lattice. We hope to extend the model in question in future works in order to link the results of statistical mechanical studies of polymerizing models and observed images for monolayers of chain fluids in the scanning tunneling microscopy experiments.

Our model is the 2D counterpart of the one proposed by Wertheim for three dimensional case in Ref. [17]. However, in our study the attractive sites are *fixed* with respect to each other in each molecule, i.e. the individual molecules are characterized by the 'valence' angle. Moreover, in contrast to the polymerizing model of Wertheim [17], the parameter of bonding length is chosen such to permit interpenetration of monomeric discs during association. This effects adds realistic features to the model. The monolayer is considered under the influence of energetic heterogeneity due to a crystalline substrate. The potentials proposed by Steele [18, 19] are used to model the fluid–solid interactions. The NVT canonical ensemble Monte Carlo simulation technique is applied to investigate the system in question. Having in mind complexity of the model, even simplified in comparison with reality, it is difficult to apply other theoretical tools than simulation techniques at present.

II. A MODEL AND PROCEDURE

Consider a one–component model for a polymerizing fluid that consists of monomeric discs each possessing two attractive intracore sites. The diameter of discs is chosen as length unit, $\sigma_f = 1$. Denote the sites on the disc i as A_i and B_i, the positions of sites inside a core are defined by vectors $\mathbf{d}_{A_i}$ and $\mathbf{d}_{B_i}$, $d = \mid \mathbf{d}_{A_i} \mid = \mid \mathbf{d}_{B_i} \mid$, each molecule is characterized by the valence angle α defined as the angle $(\mathbf{d}_{A_i}\ \mathbf{d}_{B_i})$ anticlockwise. A site represents a circle of diameter a. Denote the bonding length between centers of two discs by L.

Let us now write down the interaction between discs 1 and 2 in the form

$$U(1,2) = 0,\ r_{12} > 1 \tag{1}$$

where $r_{12} = \mid \mathbf{r}_{12} \mid$, is the center–center distance in two dimensions, $r = \sqrt{x^2 + y^2}$, and

$$U(12) = \begin{cases} -\varepsilon_{as}, & \text{for } L < r < 2d + a, \\ \text{and if} & \mid \mathbf{r}_{12} + \mathbf{d}_{A_1} - \mathbf{d}_{B_2} \mid < a \\ \text{or} & \mid \mathbf{r}_{12} + \mathbf{d}_{A_2} - \mathbf{d}_{B_1} \mid < a \\ \infty, & \text{otherwise} \end{cases}, \tag{2}$$

where ε_{as} is the association energy. Parameters of interaction, L, d and a are chosen to satisfy the condition $L < 2d + a < L + (2 - \sqrt{3})d$, to prevent double bonding of a site on one molecule with two sites on other two molecules. Throughout this work we choose the following set of parameters: $L = 0.74$, $d = 0.37$ and $a = 0.1$. This 2D model is considered within the plane which is energetically heterogenous due to a fixed distribution of underlying substrate atoms. This distribution will be chosen to correspond to (100) single crystal plane.

The interactions between fluid atoms and crystalline surfaces has been profoundly investigated by Steele [18, 19]; he proposed analytical expressions for fluid–solid potentials. These potentials arise from the summation of Lennard–Jones interactions between a given fluid particle and infinite set of atoms of the solid body. It has been shown by Steele, that the most important effect produced by a solid body on adsorbed particles comes from the atoms of the terminating solid layer.

Having this in mind we choose a following model for the fluid–solid interaction. The potential between ith fluid particle and a solid $U_{fs}(\mathbf{r}_i, z_i)$ is taken as

$$U_{fs}(\mathbf{r}_i, z_i) = \sum_{\{j\}} U_{LJ}(\rho_{ij}) \tag{3}$$

where the summation in Eq.(3) is over the atoms of one solid layer; $\mathbf{r}_i \equiv (x_i, y_i)$ is the two–dimensional vector describing the position of ith particle in laboratory frame, z_i is the position of the particle with respect to the plane where the solid atoms are located; $U_{LJ}(\rho_{ij})$ is the Lennard–Jones interaction potential between ith fluid particle and jth atom of a solid,

$$U_{LJ}(\rho_{ij}) = 4\varepsilon_{fs}[(\sigma_{fs}/\rho_{ij})^{12} - (\sigma_{fs}/\rho_{ij})^6] \tag{4}$$

and $\rho_{ij} = \sqrt{x_{ij}^2 + y_{ij}^2 + z_{ij}^2}$ is the three–dimensional vector. To simplify the model for $U_{fs}(\mathbf{r}_i, z_i)$ we consider the solid atoms to be located in $z_j = 0$ plane. Moreover, using the results of Steele [18, 19] for fluid–solid potentials we choose the plane for investigation of a polymerizing fluid to be located at a distance z_i, such to provide energetic heterogeneity of the surface for adsorbed particles of another diameter.

Therefore we use the fluid–solid potential $U(x_i, y_i, z_i)$, which implements summation of interactions of a fluid particle with an infinite one layer of solid atoms, the distance of a fluid particle w.r.t. the normal to solid atoms plane, however, is held fixed. The choice of the parameters of Lennard–Jones interactions, ε_{fs} and σ_{fs}, $\sigma_{fs} = 0.5(\sigma_f + \sigma_s)$, as well as of diameter ratio, $s_r = \sigma_f/\sigma_s$ will be discussed below.

To study the model we have applied common Metropolis Monte Carlo algorithm to obtain canonical averages for the energy and distance distributions. The simulational box has been chosen in the xy plane to be a square with length $l_x = l_y = l$. We choose the simulational box such that it contains almost 500 unit lattice cells of a crystalline lattice. Evidently the simulational box contains multiples of the unit lattice cell in x and y directions. The periodic boundary conditions have been used along these axes. The presence of surface energetic heterogeneity slightly modifies the procedure already applied for homogeneous substrate [15], the simulations for energetically heterogeneous surfaces, however, become more time consuming.

The displacement scheme applied here is a specific combination of previously used: it consists of translational and orientational displacement of each particle; if a chain is formed, we make its displacement as a whole. Actually, we have used two displacements for each individual particle, the larger one Δr_l is chosen in the interval $2\sigma_f \div 3\sigma_f$, and the smaller one, Δr_s, is approximately $0.1\sigma_f$, which is of the order of the diameter of attractive site. Orientational displacement of the particle has been performed approximately for the angle $\vartheta \simeq 130^o$, this step is done in a standard manner [20].

Displacement of chains, besides individual particles, is necessary to provide adequate sampling of the phase space in the case of formation of aggregates of particles, i.e. chains or rings. We identify the particles belonging to each chain making a member list and then displace in random direction each of chains, i.e. make simultaneous parallel translation of all members of the complex, for Δr_{ch}, $\Delta r_{ch} \simeq 2\sigma_f$. Moreover, we perform additionally displacements of chains for the distance equal to a random multiple integer of the length of unit lattice cell.

To perform orientational movements of chains, we choose arbitrarily a monomer belonging to a complex, and then all the chain is displaced orientationally w.r.t. chosen particle for the angle ϑ_{ch}. The number of attempts to displace a chain translationally and a part of it orientationally, depends on its size, i.e. on the number of monomers belonging to the chain. Each simulation step includes all the attempts to displace all the particles of the system translationally and orientationally, as well as to move, as described above, all the chains formed. The parameters of all displacements were chosen such to provide reasonable partial acceptance ratios for each type of displacements and total acceptance ratio. In all the runs performed, partial acceptances have been $30 \div 50\%$ which in conjunction yield stable total acceptance ratio around 20%.

The systems considered on the almost homogeneous and energetically heterogeneous surfaces were equilibrated for at least 4×10^4 of simulational steps. Acceptance ratio in the runs with homogeneous and heterogeneous surfaces was almost equal. A productive run, during which the averages were obtained, consisted of not less than $(1.2 \div 1.5) \times 10^5$ steps. Energetic criterium has been used to determine if equilibration had been reached. For systems on ideal surface the fluctuations of energy per particle were less than 5%, however, in the presence of energetic heterogeneity the fluctuations become slightly stronger, we assume that equilibration has been reached if the the fluctuations of energy are less than 8%.

We perform thorough analysis of bonded configurations of particles and all other averages which characterize the bulk polymerizing fluid. Our main concern is a comparison of the formation of chains due to chemical association on an ideal surface and crystalline surfaces.

III. RESULTS AND DISCUSSION

Very recently we have investigated the model for polymerizing fluid in question on the ideal surface, i.e. energetically homogeneous plane [15]. Now, our main concern is the influence of energetic heterogeneity of the surface. From the variety of lattices, in this study we have chosen a square lattice which correspond to (100) single crystal plane. A slightly more complicated case of (111) lattice will be considered elsewhere, with an emphasis on the systems related more closely to particular molecules of experimental interest.

The (100) single crystal surface is a square lattice with unit cell length σ_s. The unit lattice cell is characterized by atom positions $(a) : (0,0)$, $(0,\sigma_s)$, $(\sigma_s, 0)$, (σ_s,σ_s), by adsorbing site position (s) - $(0.5\sqrt{2}\sigma_s, 0.5\sqrt{2}\sigma_s)$, and saddle point positions $(sp) : (0, 0.5\sigma_s)$, $(0.5\sigma_s, 0)$, $(\sigma_s, 0.5\sigma_s)$, $(0.5\sigma_s, \sigma_s)$. The diameter of fluid particles is chosen to be smaller than the diameter of solid atoms, such that $\sigma_f/\sigma_s = 2/3$. Adsorbing plane in this case has been chosen to be located at $z/\sigma_s = 0.67$, i.e. at a distance which yields sufficient energetic heterogeneity for polymerizing particles as it follows from the calculations performed by Steele, see e.g. Refs.[18, 19]. The energy of Lennard–Jones fluid–solid interaction varies from $\beta\varepsilon_{fs} = 0$ (homogeneous surface) to $\beta\varepsilon_{fs} = 1.5$ (strongly heterogeneous surface). Evidently, the external periodic field influences statistics of bonding states of particles and all the features of polymerization in the monolayer.

We have performed simulations for two different values of the density of discs: $\rho = 0.4$ and $\rho = 0.6$. Two values of association energy are investigated: $\beta\varepsilon_{as} = 10$ and $\beta\varepsilon_{as} = 15$, to provide comparison of the structure of the monomolecular layer on ideal and crystalline surface. The valence angle α, is chosen to be 135°, 160°, 180°. We will begin with discussion of the case $\alpha = 135°$, similarly to our previous work [15]. With this value, one would expect the formation of rings made of eight monomers as follows from geometric arguments. The formation of rings of eight elements has been involved in the explanation of experiments on the structure of liquid sulphur [21, 22] and its changes with temperature. The model in question is characterized, however, by the attractive sites of finite diameter, therefore rings that are formed due to association can be polydisperse (they can contain different number of particles).

Before proceeding with the description of the results let us introduce some notations. To perform simulations in each case we consider N particles in the simulation square cell with area S. We have calculated the average concentrations of singly bonded and doubly bonded particles $X_1 = N_1/N$ and $X_2 = N_2/N$ (N_i, $i = 1,2$ is the number of i–bonded particles) in the unit lattice cell. The fraction of unbounded species X_0 is then straightforwardly determined, $X_0 = 1 - X_1 - X_2$. Some of our results, such as the density profiles, the pair distribution functions, the structure factors, will be presented in graphical form, all other are collected and given in tables.

We would like to discuss five effects of interest in the behavior of the monolayer on heterogeneous substrate, namely the effect of the density of discs, of association energy, of the valence angle value and of substrate heterogeneity.

The effect of surface energetic heterogeneity and of association energy between discs is discussed according to the data presented in Table 1. Here we investigate the case of intermediate disc density, $\rho = 0.4$. For lower value of association energy, $\beta\varepsilon_{as} = 10$, the fraction of singly bonded particles increases with increasing fluid–solid energy, i.e. with surface energetic corrugation, a maximum of X_1 is observed at $\beta\varepsilon_{fs} = 1$, for still augmenting fluid–solid energy X_1 decreases. The fraction of doubly bonded particles behaves differently, it exhibits maximum value at low fluid–solid energy, $\beta\varepsilon_{fs} = 0.2$, and then decreases with increasing $\beta\varepsilon_{fs}$. Consequently the fraction of unbounded species increases quite slowly for low fluid energies and then augments more rapidly with increasing fluid–solid energy — this is a very clear manifestation of the disordering effect of crystalline lattice energetic heterogeneity on the association phenomena in the monolayer at this density, $\rho = 0.4$. For higher value of association energy between discs, $\beta\varepsilon_{as} = 15$, the fraction of singly bonded discs increases whereas X_2 decreases with increasing substrate corrugation. The number of free monomers in the case $\beta\varepsilon_{as} = 15$ is lower than for $\beta\varepsilon_{as} = 10$ for all corrugations, as expected. Saturation of the monomer number for augmenting corrugation also is observed at $\beta\varepsilon_{as} = 15$.

To proceed, we denote by n_{ch} and n_{rg} the number of chains and rings that are formed due to association in the monolayer, respectively. Chains and rings contain m_{ch} and m_{rg} particles, respectively. Irrespectively to the number of dimers and of monomers belonging to higher order complexes (chains and rings) we conclude from the data given in Table 1, for $\beta\varepsilon_{as} = 10$, that the mean numbers of chains and rings, $\langle n_{ch}\rangle$ and $\langle n_{rg}\rangle$, respectively, attain maxima at the same values of the fluid–solid energy to those at which $X_1$and X_2 have maxima. The average number of chains is overwhelmingly larger than that of rings, as expected. For higher association energy, $\beta\varepsilon_{as} = 15$, the number of chains increases, following increasing X_1. However, the number of rings has maximum at surface corrugation, $\beta\varepsilon_{fs} = 0.5$, it follows that $\langle n_{rg}\rangle$ is specific w.r.t. the corrugation energy values for the model in question.

$\varepsilon_{sf}/kT =$	0.	0.2	0.5	1.	1.5
$\langle X_1\rangle_{10}$	$0.25 \pm 3\%$	$0.37 \pm 5\%$	0.45 ± 6	$0.51 \pm 6\%$	$0.44 \pm 3\%$
$\langle X_1\rangle_{15}$	$0.22 \pm 3\%$	$0.33 \pm 4\%$	0.42 ± 2	$0.43 \pm 5\%$	$0.44 \pm 2\%$
$\langle X_2\rangle_{10}$	$0.35 \pm 4\%$	$0.58 \pm 4\%$	$0.46 \pm 8\%$	$0.36 \pm 7\%$	$0.27 \pm 4\%$
$\langle X_2\rangle_{15}$	$0.38 \pm 4\%$	$0.66 \pm 4\%$	$0.54 \pm 3\%$	$0.45 \pm 5\%$	$0.45 \pm 5\%$
$\langle n_{ch}\rangle_{10}$	$48.6 \pm 5\%$	$63 \pm 6\%$	$85 \pm 5\%$	$89.5 \pm 3\%$	$81. \pm 8\%$
$\langle n_{ch}\rangle_{15}$	$40 \pm 5\%$	$55 \pm 4\%$	$75 \pm 4\%$	$77 \pm 4\%$	$78.1 \pm 3\%$
$\langle n_{rg}\rangle_{10}$	$0.9 - 1.2$	$0.9 - 1.6$	$0.6 - 0.9$	$0.5 - 0.7$	$0.4 - 1.1$
$\langle n_{rg}\rangle_{15}$	$1 - 1.6$	$0.3 - 0.9$	$1.1 - 1.8$	$0.7 - 1.2$	$0.5 - 0.7$
$\langle m_{ch}\rangle_{10}$	$4.93 \pm 4\%$	$5.3 \pm 6\%$	$4. \pm 5\%$	$3.4 \pm 6\%$	$3.1 \pm 5\%$
$\langle m_{ch}\rangle_{15}$	$4.9 \pm 4\%$	$6.1 \pm 3\%$	$4.5 \pm 3\%$	$4 \pm 5\%$	$4.1 \pm 5\%$
$\langle m_{rg}\rangle_{10}$	$6.7 - 7.1$	$6 - 7.2$	$6 - 6.5$	$5.5 - 6$	$6 - 6.3$
$\langle m_{rg}\rangle_{15}$	$6.7 - 7.6$	$6.4 - 7.1$	$6.8 - 7$	$6.8 - 7$	$6.7 - 7$
$\langle R_g^2\rangle_{10}$	$10.2 \pm 6\%$	$10.8 \pm 6\%$	$10.6 \pm 6\%$	$9.2 \pm 4\%$	$6 \pm 5\%$
$\langle R_g^2\rangle_{15}$	$11.3 \pm 5\%$	$13.5 \pm 7\%$	$12 \pm 5\%$	$10 \pm 6\%$	$9.8 \pm 4\%$
$\langle r_{ee}^2\rangle_{10}$	$2.5 \pm 2\%$	$3.4 \pm 1\%$	$2.6 \pm 4\%$	$2.25 \pm 4\%$	$1.9 \pm 5\%$
$\langle r_{ee}^2\rangle_{15}$	$2.7 \pm 2\%$	$3.5 \pm 3\%$	$2.9 \pm 5\%$	$2.6 \pm 7\%$	$2.7 \pm 4\%$
$\langle l_p\rangle_{10}$	$0.8 \pm 4\%$	$0.73 \pm 8\%$	$1.1 \pm 7\%$	$1.15 \pm 6\%$	$1.14 \pm 5\%$
$\langle l_p\rangle_{15}$	$0.69 \pm 4\%$	$0.52 \pm 4\%$	$0.94 \pm 5\%$	$1.02 \pm 1\%$	$1 \pm 1\%$

Table 1. The MC simulation results for associative disks with valence angle $\alpha = 135^o$ on the 100–lattice; $\rho = 0.4$, $\varepsilon_{as}/kT = 10$ and $\varepsilon_{as}/kT = 15$.

At $\beta\varepsilon_{as} = 10$, the average number of monomers in chains is around 5 for low values of $\beta\varepsilon_{fs}$, then $\langle m_{ch}\rangle$ decreases; this behavior also is observed at $\beta\varepsilon_{as} = 15$, just the values for $\langle m_{ch}\rangle$ are larger for all corrugations, in comparison with $\beta\varepsilon_{as} = 10$. In the case of rings formed due to association we merely state that they are polydisperse — rings made of 6, 7 and 8 elements contribute to $\langle m_{rg}\rangle$, rings consisting of 8 monomers are formed, however, only for low fluid–solid energy, for high values of $\beta\varepsilon_{fs}$ we observe that $\langle m_{rg}\rangle$ is equal or smaller than 7.

Let us introduce some definitions, necessary to complement our description of associates formed in the monolayer. To describe quantitatively chains that are formed due to association, we define, as usual, the mean square end to end distance

$$r_{ee}^2 = \frac{1}{n_{ch}} \sum_{1<i<n_{ch}} (r_1^i - r_e^i)^2, \tag{5}$$

where r_1^i and r_e^i are the coordinates of the first and last particles in the chain i, respectively. The values for averaged r_{ee}^2, $\langle r_{ee}^2\rangle$ in (100) case for different values of $\beta\varepsilon_{fs}$ are given in Table 1. Evidently, rings do not contribute to the $\langle r_{ee}^2\rangle$ value.

We would like now to define the mean square radius of gyration assuming that all the particles belonging to chains or rings are of equal mass, $m = 1$, as follows:

$$R_g^2 = \frac{1}{(n_{ch}+n_{rg})}\left(\sum_{1<j<n_{ch}} \frac{1}{m_{ch}^j} \sum_{1<i<m_{ch}^j} (r_i^j - R_c^j)^2 + \sum_{1<j<n_{rg}} \frac{1}{m_{rg}^j} \sum_{1<i<m_{rg}^j} (r_i^j - R_c^j)^2\right), \tag{6}$$

where R_c^j denote the coordinates of the center of mass of a chain or ring j. Finally define the persistence length, l_p for complexes formed due to association, it includes chains and rings. The persistence length is defined as follows:

$$l_p = \frac{1}{(n_{ch}+n_{rg})}[\sum_{1<j<n_{ch}} \sum_{1<i<m_{ch}-1} (\mathbf{b}_1^j \mathbf{b}_i^j) \mid \mathbf{b}_i^j \mid + \sum_{1<j<n_{rg}} \sum_{1<i<m_{rg}-1} (\mathbf{b}_1^j \mathbf{b}_i^j) \mid \mathbf{b}_i^j \mid], \tag{7}$$

where $\mathbf{b}_i^j = \mathbf{r}_i^j - \mathbf{r}_{i+1}^j$ is the vector determining orientation of i bond in the cluster j. The values for averaged persistence length $\langle l_p \rangle$ also are given in Table 1.

We observe, for both association energies in question, that $\langle r_{ee}^2 \rangle$ has maximum value at $\beta\varepsilon_{fs} = 0.2$ and next, with increasing fluid–solid energy, $\langle r_{ee}^2 \rangle$ decreases. This behavior should be expected, because the $\langle m_{ch} \rangle$ maximum is observed at this fluid–solid energy and $\langle r_{ee}^2 \rangle$ is the averaged individual property of a chain molecule formed due to association. With chosen value of valence angle, $\alpha = 135°$, the values for $\langle r_{ee}^2 \rangle^{1/2}$are low, because chain molecules are not extended. The mean square radius of gyration decreases with increasing substrate corrugation for both values of association energy, $\beta\varepsilon_{as} = 10$ and $\beta\varepsilon_{as} = 15$. The averaged persistence length, $\langle l_p \rangle$, is higher for higher values of $\beta\varepsilon_{fs}$ but is less affected (comparatively to other properties) by changes of $\beta\varepsilon_{fs}$ in this region of values of fluid–solid energy, as a result of not too large changes of the number of chains and their average length.

For the sake of better visualization we present in Figs. 1a and 1b, as an example, the snapshots of the final configuration of particles in the simulation cell at $\beta\varepsilon_{as} = 10$, for $\beta\varepsilon_{fs} = 0.2$ and for $\beta\varepsilon_{fs} = 1.5$, respectively. "Dis–associating" effect for increasing fluid–solid energy can be seen from these figures.

We would like now to discuss quantitative features of the influence of the valence angle parameter on the structure of the monolayer. We have performed two runs for the model at $\rho = 0.4$, $\beta\varepsilon_{as} = 15$, $\alpha = 160^o$ for corrugations $\beta\varepsilon_{fs} = 0.2$ and $\beta\varepsilon_{fs} = 1.5$ and two more runs for similar conditions, but for the model $\alpha = 180^o$. For larger angles than $\alpha = 135^o$, one would expect the formation of more extended structures (rings must become less probable) and longer chains with higher probability. From the data presented in Table 2, we observe that the numbers of singly and doubly bonded particles, X_1 and X_2, are almost equal for the models with $\alpha = 135°$, $160°$, and $\alpha = 180°$ at given surface corrugation $\beta\varepsilon_{fs} = 0.2$ and $\beta\varepsilon_{fs} = 1.5$. Higher surface corrugation yields lower fraction of doubly bonded species whereas the fraction of singly bonded species increases. The average number of chains is also weakly sensitive to changes of the valence angle and less depend on α than on surface corrugation. However, for less heterogeneous surface, $\beta\varepsilon_{fs} = 0.2$, the number of chains slightly increases for $\alpha = 180°$ in comparison with $\alpha = 135°$, whereas for a stronger heterogeneous surface, $\beta\varepsilon_{fs} = 1.5$, the number of chains slightly decreases for $\alpha = 180°$ comparing with $\alpha = 135°$. Higher $\beta\varepsilon_{fs}$ — shorter chains are more probable to form. The average number of monomers is evidently influenced by the value of valence angle, it is slightly larger for models with $\alpha = 160°$ and $\alpha = 180°$ than $135°$.

a

b

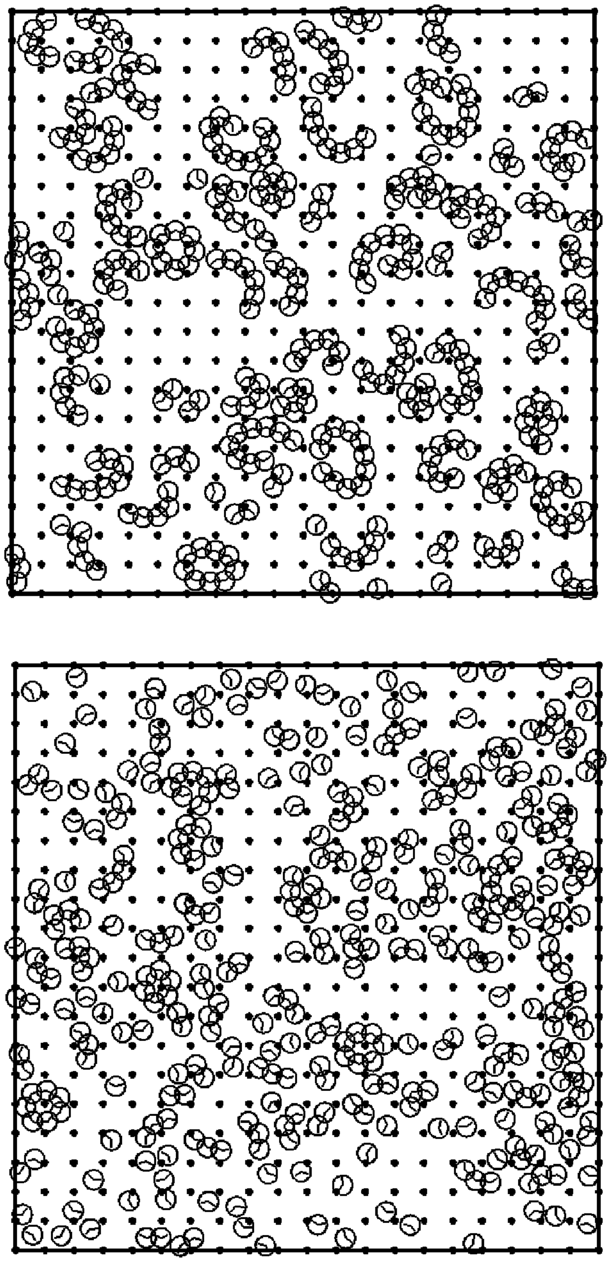

Fig. 1. Snapshots of the final configuration of particles in the simulation square for the model $\alpha = 135^o$ at $\rho = 0.4$, $\beta\varepsilon_{as} = 10$, $\beta\varepsilon_{fs} = 0.2$ (part a) and at $\beta\varepsilon_{fs} = 1.5$ (part b).

$\varepsilon_{sf}/kT =$	0.	0.2	1.5
	$\alpha = 180^o$		
$\langle X_1\rangle_{15}$	$0.32 \pm 2\%$	$0.317 \pm 4\%$	$0.418 \pm 3\%$
$\langle X_2\rangle_{15}$	$0.63 \pm 4\%$	$0.65 \pm 4\%$	$0.5 \pm 3\%$
$\langle n_{ch}\rangle_{15}$	$58.4 \pm 3\%$	$57.1 \pm 4\%$	$75.3 \pm 4\%$
$\langle m_{ch}\rangle_{15}$	$5.95 \pm 2\%$	$6.17 \pm 2\%$	$4.35 \pm 3\%$
$\langle R_g^2\rangle_{15}$	$16.2 \pm 4\%$	$15.4 \pm 5\%$	$9.71 \pm 4\%$
$\langle r_{ee}^2\rangle_{15}$	$18.75 \pm 4\%$	$18.05 \pm 4\%$	$8.78 \pm 5\%$
$\langle l_p\rangle_{15}$	$3.06 \pm 4\%$	$3.35 \pm 4\%$	$2.52 \pm 3\%$
	$\alpha = 160^o$		
$\langle X_1\rangle_{15}$	$0.33 \pm 3\%$	$0.31 \pm 5\%$	$0.43 \pm 3\%$
$\langle X_2\rangle_{15}$	$0.61 \pm 4\%$	$0.66 \pm 3\%$	$0.48 \pm 4\%$
$\langle n_{ch}\rangle_{15}$	$60 \pm 3\%$	$56 \pm 4\%$	$77.2 \pm 4\%$
$\langle m_{ch}\rangle_{15}$	$5.7 \pm 3\%$	$6.35 \pm 3\%$	$4.26 \pm 3\%$
$\langle R_g^2\rangle_{15}$	$13.6 \pm 4\%$	$16.3 \pm 4\%$	$9.74 \pm 3\%$
$\langle r_{ee}^2\rangle_{15}$	$8.1 \pm 5\%$	$11 \pm 4\%$	$5.8 \pm 4\%$
$\langle l_p\rangle_{15}$	$1.6 \pm 3\%$	$1.86 \pm 4\%$	$1.82 \pm 4\%$

Table 2. The MC simulation results for associative disks with valence angles $\alpha = 160^o$ and $\alpha = 180^o$ on the 100–lattice; $\rho = 0.4$, $\varepsilon_{as} = 15$.

We conclude that the effect of surface corrugation is more important than that of valence angle for the models in question, i.e. restricted to α from 135^o to 180^o, for the values of association energy considered. Both for mean square end to end distance and for persistence length we observe trends of behavior which can be explained by a more probable formation of extended structures for the model with $\alpha = 180°$ comparing with $\alpha = 135°$. However, the averaged square radius of gyration is more sensitive to the number of chains and number of participants in them dependencies on valence angle. $\langle R_g^2\rangle$ slightly decreases for augmenting α at high surface corrugation whereas for $\beta\varepsilon_{fs} = 0.2$ it behaves nonmonotonously with α.

It follows from the data for $\langle n_{ch}\rangle$ and $\langle n_{rg}\rangle$, which describe the number of chains and rings irrespectively to the number of monomers belonging to them, that the number $\langle n_{ch}\rangle + \langle n_{rg}\rangle$ is lower for $\beta\varepsilon_{as} = 15$, than for $\beta\varepsilon_{as} = 10$. However, the average number of monomers belonging to chains and to rings, $\langle m_{ch}\rangle$ and $\langle m_{rg}\rangle$, respectively, is higher for the case $\beta\varepsilon_{as} = 15$, than for $\beta\varepsilon_{as} = 10$. Thus, chains and rings that are formed, are longer and larger, respectively, for a higher association energy at given value of surface energetic heterogeneity. From a comparison of the results for $\langle r_{ee}^2\rangle$ presented in Table 1 and Table 2 we conclude that chains formed due to association at $\beta\varepsilon_{as} = 15$ are characterized by a slightly larger $\langle r_{ee}^2\rangle$ than at $\beta\varepsilon_{as} = 10$, however trends of behavior of $\langle r_{ee}^2\rangle$ with increasing fluid–solid energy $\beta\varepsilon_{fs}$ are qualitatively similar.

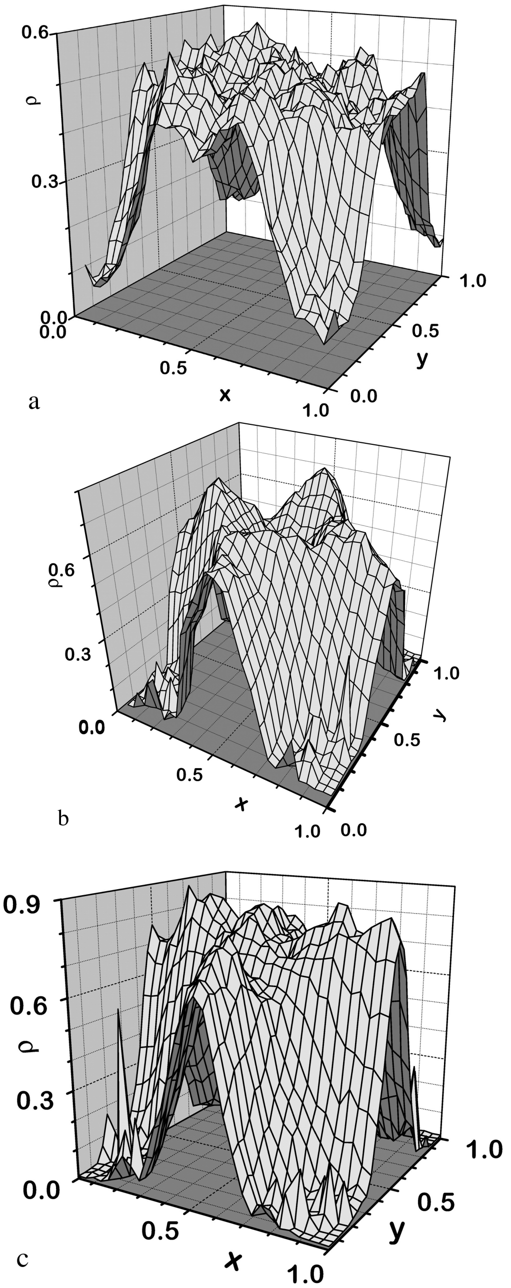

Fig. 2. The three–dimensional plots of the local disc density over unit lattice cell of the (100) single crystal plane, $\rho(x, y)$, in the monolayer of polymerizing hard spheres at density $\rho = 0.4$. The association energy $\beta\varepsilon_{as}$ is 10 (part a) and $\beta\varepsilon_{as}$ equals to 15 in parts b and c. The energy of fluid–solid interaction $\beta\varepsilon_{fs}$ is 0.2 (part a) and 1.5 (parts b and c). Parts a and b refer to the model with the valence angle $\alpha = 135^o$, whereas part c refers to the valence angle $\alpha = 180^o$.

The values for average persistence length depend on $\beta\varepsilon_{fs}$ in similar way for both association energies. Due to a larger values for $\langle m_{ch}\rangle$ in the case $\beta\varepsilon_{as} = 15$ we observe slightly higher $\langle l_p\rangle$ values, in comparison with $\beta\varepsilon_{as} = 10$ at a given $\beta\varepsilon_{fs}$. However, a higher surface heterogeneity opposes stronger to the formation of complexes in the monolayer.

Finally we would like to discuss quantitatively the effect of disc density at different corrugations on the structure of the monolayer. Simulation runs for $\rho = 0.6$ have been performed for the model with $\alpha = 135°$ at $\beta\varepsilon_{as} = 10$, for $\beta\varepsilon_{fs} = 0.2$ and for $\beta\varepsilon_{fs} = 1.5$ (the corresponding data have been collected in Table 3). General trends are that the number of doubly bonded particles is larger for $\rho = 0.6$ than at lower density $\rho = 0.4$. The average length of chains also is larger for a higher density. The surface corrugation evidently yields a dissociating effect that competes with chemical association mechanism.

Let us discuss now the structure of the monolayer at different conditions. We start from the case: $\rho = 0.4$, $\beta\varepsilon_{as} = 15$, $\alpha = 135°$, and discuss the structure of the monolayer in terms of the density distributions over the unit lattice cell and of the pair distribution functions (pdfs). In Figs. 2a and 2b we present a three–dimensional plots of the local disc density $\rho(x, y)$ over the unit lattice cell of the (100) single crystal surface at $\beta\varepsilon_{fs} = 0.2$ and $\beta\varepsilon_{fs} = 1.5$, respectively. In contrast to the behavior of unassociated fluid (in that case one would expect higher density over s position, lower density of particles over sp positions and finally negligibly small density over atom positions, a, for associating fluid over the unit cell we observe density distribution which is determined by association effects rather than by surface heterogeneity. However, at a high value of association energy, $\beta\varepsilon_{as} = 15$, the bonded structures are not constrained much for low external field corrugation ($\beta\varepsilon_{fs} = 0.2$), see Fig. 2a. In contrast, for high corrugation ($\beta\varepsilon_{fs} = 1.5$) there is a minimum at the adsorbing site position. The density distribution is affected by corrugation such that bonded structures attain preferable orientations (Fig. 2b). If the valence angle changes to $\alpha = 180°$ with other parameters unchanged the density distribution over unit lattice cell changes, straight chains seem to be less restricted to move; the density minimum in the adsorbing site position practically disappears.

To get a deeper insight into this distribution we show in Fig. 3a the local density behavior at $\beta\varepsilon_{as} = 10$, $\beta\varepsilon_{fs} = 0.2$ and at $\beta\varepsilon_{fs} = 1.5$ along the edge of the unit lattice cell, ($a - sp - a$ line) and along midline of the cell, $sp - s - sp$, in Fig. 3b we present similar data but at $\beta\varepsilon_{as} = 15$. It follows from Fig. 3a, that local density distribution of particles is heterogeneous, it is improbable to find particles over atom positions whereas over sp position of the unit cell the density is much higher. It augments with increasing surface corrugation. Smaller corrugation — smoother distribution of density along $sp - s - sp$ direction.

$\langle X_1\rangle_{10}$	$0.25 \pm 2\%$	$0.3 \pm 3\%$	$0.39 \pm 3\%$
$\langle X_2\rangle_{10}$	$0.72 \pm 4\%$	$0.59 \pm 3\%$	$0.53 \pm 4\%$
$\langle n_{ch}\rangle_{10}$	$68 \pm 3\%$	$98 \pm 4\%$	$104 \pm 4\%$
$\langle n_{rg}\rangle_{10}$	$0.6 - 1.2$	$2 - 3.8$	$3.2 - 3.7$
$\langle m_{ch}\rangle_{10}$	$7.7 \pm 3\%$	$5 \pm 2\%$	$4.7 \pm 3\%$
$\langle m_{rg}\rangle_{10}$	$9 - 9.5$	$7.1 - 7.8$	$6.8 - 7$
$\langle R_g^2\rangle_{10}$	$15.5 \pm 6\%$	$11 \pm 5\%$	$13.8 \pm 6\%$
$\langle r_{ee}^2\rangle_{10}$	$3.3 \pm 5\%$	$3 \pm 4\%$	$2.7 \pm 4\%$
$\langle l_p\rangle_{10}$	$0.5 \pm 4\%$	$0.84 \pm 4\%$	$0.88 \pm 6\%$

Table 3. The MC simulation results for associative disks with valence angle $\alpha = 135^o$ on the 100–lattice; $\rho = 0.6$, $\varepsilon_{as} = 10$.

From the curves of the density distribution given in both parts of Fig. 3 in conjunction, it follows that associated species most probably orient along $sp - s - sp$ direction in the unit cell, chain–like structure "grows" preferably such that sp and s positions become occupied. Larger fluid–solid energy yields larger difference of densities along different directions, such that a set of orientations of associated species become more restricted.

The in–plane pair distribution function of particles, $g(r)$, averaged over the positions of one particle (it is chosen as reference point) in the simulation shell, is more structured at intermediate interparticle separations at $\beta\varepsilon_{fs} = 1.5$, in comparison with $\beta\varepsilon_{fs} = 0.2$, Fig. 4a. For a lower value of fluid–solid energy, $\beta\varepsilon_{fs} = 0.2$, the pdf is characterized by a substantially higher first maximum, in comparison with the case of a higher surface heterogeneity, $\beta\varepsilon_{fs} = 1.5$. On the other hand the effect of augmenting association energy yields higher first maximum and more pronounced correlations between fluid particles at intermediate distances (Fig. 4b).

The value of the valence angle also influences the pair distribution functions (Fig. 5). Chains that are more straight on average ($\alpha = 180°$) are characterized by the pdf with higher maxima in comparison with the case of lower valence angle ($\alpha = 160°$). The effect of surface corrugation is very similar to that observed for the model with $\alpha = 135°$, cf. Fig. 4.

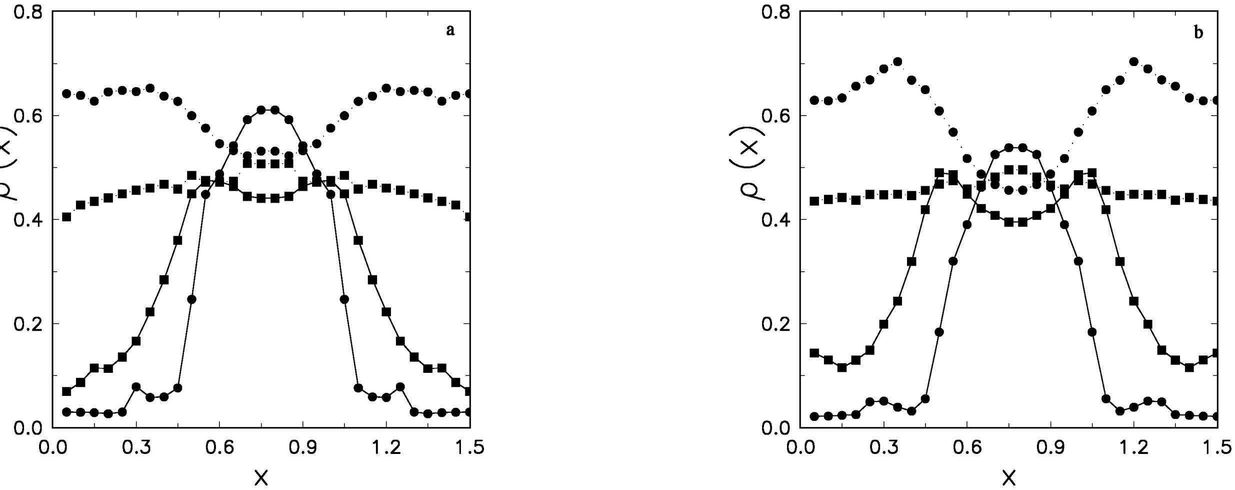

Fig. 3. The averaged density profiles of discs over unit lattice cell of (100) lattice along the edge $a-sp-a$ and along $sp-s-sp$ direction. The squares and circles are for $\beta\varepsilon_{fs}=0.2$ and for $\beta\varepsilon_{fs}=1.5$, respectively. The lower line with each kind of symbols is for $a-sp-a$ direction, whereas the upper line is for $sp-s-sp$ direction. The fluid density is $\rho=0.4$; $\alpha=135^{o}$. In part a the association energy $\beta\varepsilon_{as}$ is 10 whereas in part b $\beta\varepsilon_{as}$ is 15.

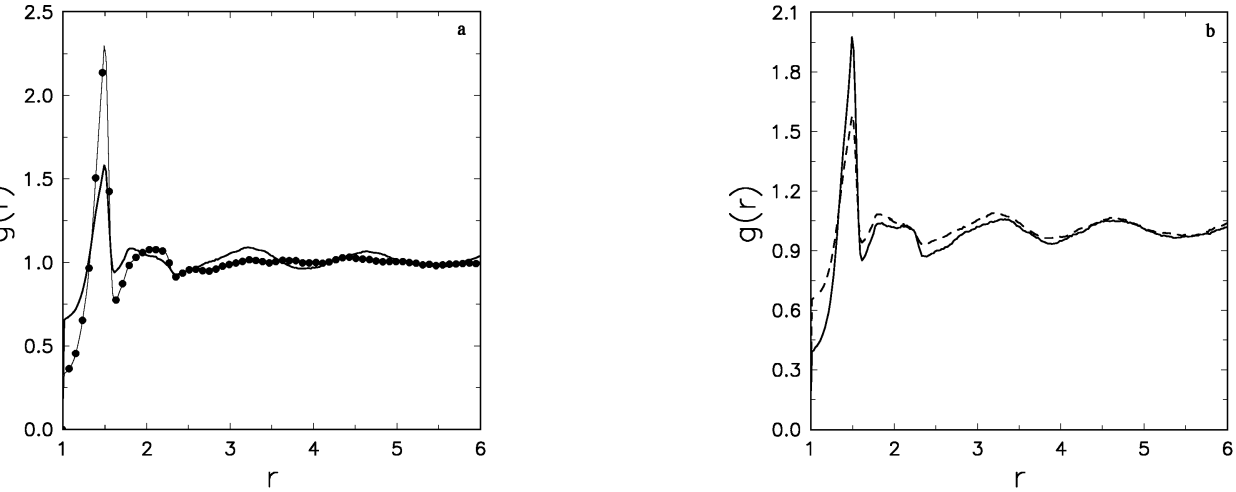

Fig. 4. The pair distribution functions of fluid particles for $\beta\varepsilon_{fs}=1.5$ (solid thick line) and for $\beta\varepsilon_{fs}=0.2$ (thin line with circles), part a. The association energy $\beta\varepsilon_{as}$ is 10 in this panel. In part b the association energy $\beta\varepsilon_{as}$ is 10 (dashed line) and $\beta\varepsilon_{as}$ is 15 (solid line). The surface corrugation is $\beta\varepsilon_{fs}=1.5$ in part b. The fluid density is $\rho=0.4$; $\alpha=135^{o}$.

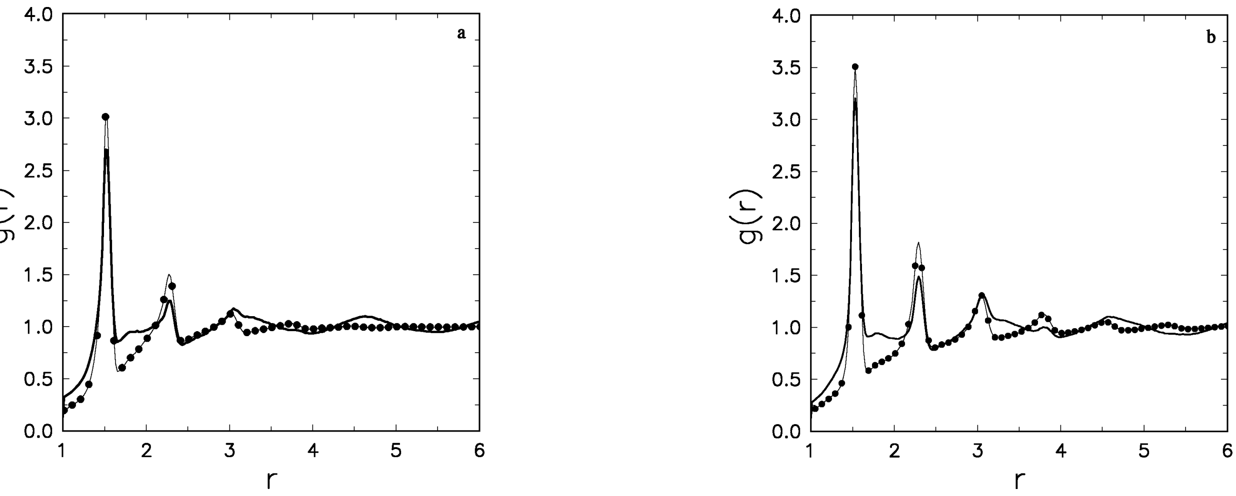

Fig. 5. The pair distribution functions of fluid particles for $\beta\varepsilon_{fs}=1.5$ (solid thick line) and for $\beta\varepsilon_{fs}=0$ (thin line with circles), part a. The association energy $\beta\varepsilon_{as}$ is 15 and the valence angle is $\alpha=160^{o}$, in this panel. In part b we present similar data, but for the model with valence angle $\alpha=180^{o}$. The fluid density is $\rho=0.4$ in both parts of the figure.

IV. CONCLUSIONS

The canonical ensemble Monte Carlo simulations are reported in this work for chemically associating two–dimensional fluids which can polymerize for certain interaction energies, due to the presence of two attractive sites per monomeric hard disc. The fluids are considered to form a monolayer on the crystalline lattice of (100) symmetry. We have obtained that the surface energetic heterogeneity plays an important role in the distributions of fluid density over unit lattice cell. Surface corrugation yields that the associated species preferably attain configurations along saddle point — adsorbing site — saddle point positions. Stronger corrugation results in a smaller first maximum of the pair distribution function of the fluid species but in more pronounced correlations at intermediate distances between fluid particles. Higher value of association energy yields longer individual chain–like structures and a larger number of chains. The number of rings that can be formed in the model with valence angle $\alpha = 135°$ appeared to be very small, even for high values of the association energy and sufficiently high fluid density. It seems that cooperative effects, such as three–body interactions, are necessary to involve for the generation of rings via the chemical association mechanism. We have analyzed in detail the fractions of singly and doubly bonded particles and have observed that each fraction saturates at certain value of fluid density. Our results can be of interest for the development of theoretical approaches for the structure and thermodynamics of monolayers of chain molecules. Having in mind existing experimental possibilities for the visualization of the monolayer structure it would be important to extend our study for the case of a more sophisticated internal structure of fluid molecules.

ACKNOWLEDGMENTS

This work was supported in parts by Silicon Graphics Inc. – Cray Research of Mexico under its University Research and Development Grant program, by CONACyT of Mexico under grant 25301E and by DGAPA of the UNAM under the project IN111597. We are grateful to the Departamento de Supercomputo of the UNAM for allocation of computer time on the Origin 2000 computer.

[1] J. P. Rabe, S. Buchholz, Science **253**, 424 (1991).
[2] A. M. Baro, R. Miranda, J. Alaman *et al.*, Nature **315**, 253 (1985).
[3] G. Watel, F. Thibaudau, J. Cousty, Surf. Sci. Lett. **281**, L297 (1993).
[4] L. Askadskaja, J. P. Rabe, Phys. Rev. Lett. **69**, 1395 (1992).
[5] G. C. McGonigal, R. H. Bernhardt, D. J. Thomson, Appl. Phys. Lett. **57**, 28 (1990).
[6] M. Sprik, E. Delamarche, B. Michel *et al.*, Langmuir **10**, 4116 (1994).
[7] E. Helfand, H. L. Frisch, J. L. Lebowitz, J. Chem. Phys. **34**, 1031 (1961).
[8] W. A. Steele, J. Chem. Phys. **65**, 5256 (1976).
[9] D. Henderson, Mol. Phys. **34**, 301 (1977).
[10] T. Boublik, Mol. Phys. **63**, 685 (1988).
[11] E. D. Glandt, D. D. Fitts, J. Chem. Phys. **66**, 4503 (1977).
[12] K. Bagchi, H. C. Andersen, W. Swope, Phys. Rev. E **53**, 3974 (1996).
[13] Y. Zhou, C. K. Hall, G. Stell, J. Chem. Phys. **103**, 2688 (1995).
[14] D. Henderson, A. Huerta, O. Pizio, A. Trokhymchuk, Mol. Phys. **90**, 571 (1997).
[15] Yu. Duda, A. Trokhymchuk, S. Sokolowski, O. Pizio, J. Coll. Interface Sci. **194**, 68 (1997).
[16] O. Pizio, Yu. Duda, A. Trokhymchuk, S. Sokolowski, J. Mol. Liq. **76**, 813 (1998).
[17] M. S. Wertheim, J. Chem. Phys. **87**, 7323 (1987).
[18] W. A. Steele, Surf. Sci. **36**, 317 (1973).
[19] W. A. Steele, *The Interaction of Gases with Solid Surfaces* (Pergamon, Oxford, 1974).
[20] M. P. llen, D. J. Tildesley, *Computer Simulations of Liquids* (Clarendon, Oxford, 1987).
[21] R. Bellisent, L. Descotes, F. Boue, P. Pfeuty, Phys. Rev. B **41**, 2135 (1990).
[22] R. Bellisent, L. Descotes, P. Pfeuty, J. Phys.: Cond. Matt. **6**, A211 (1994).

ДОСЛІДЖЕННЯ МЕТОДОМ МОНТЕ–КАРЛО МОНОМОЛЕКУЛЯРНОЇ ПЛІВКИ ХЕМІЧНО АСОЦІЯТИВНОГО ПОЛІМЕРИЗАЦІЙНОГО ФЛЮЇДУ, АДСОРБОВАНОГО НА КРИСТАЛІЧНІЙ ПОВЕРХНІ

Ю. Дуда[1,*], О. Пізіо[1], С. Соколовскі[2], Н. Батіна[3]
[1] *Інститут хемії, Мексиканський національний автономний університет, Койоакан, 04510, Мехіко, Мексика*
[2] *Комп'ютерна лабораторія, факультет хемії, Університет Марії Кюрі–Склодовської, 203–31, Люблін, Польща*
[3] *Факультет фізики, Автономний університет Метрополітана/Iзтапалапа, 09430, Мехіко, Мексика*
[*] *Постійна адреса: Інститут фізики конденсованих систем НАН України, вул. Свєнціцького, 1, Львів, 290011, Україна*

Розглядаємо модель мономолекулярної плівки полімеризованого флюїду, адсорбованого на кристалічній поверхні. Використано метод комп'ютерного експерименту Монте–Карло в NVT ансамблі. Флюїд моделюється твердими дисками, що можуть утворювати полімерні ланцюжки завдяки притяганню між їхніми допоміжними силовими центрами. Досліджено, як валентний кут та енергія асоціятивної взаємодії впливають на формування структури моношару в заданому зовнішньому полі кристалічної ґратки. Для оцінки впливу кристалічної поверхні на структуру адсорбовані плівки проведено комп'ютерний експеримент для різних величин взаємодії атомів флюїду з атомоми поверхні. Здійснено аналіз величин асоціятивних комплексів, що сформувалися на поверхні (ланцюгів та кілець), а також наведені концентрації одно– та двозв'язних атомів флюїду. Пораховано усереднену відстань між кінцями ланцюга та радіус ґірації, проаналізовано залежність цих величин від геометричних параметрів та параметрів взаємодії.